

Research Article

Evaluating the Effects of Chemical Composition on Induction Heating Ability of Fe_2O_3 -CaO-SiO₂ Glass Ceramics

Y. Y. Wang, B. Li, Y. L. Yu, and P. S. Tang

Department of Material Chemistry, Huzhou University, Huzhou 313000, China

Correspondence should be addressed to Y. Y. Wang; arince@hutczj.cn

Received 27 October 2015; Revised 1 March 2016; Accepted 21 March 2016

Academic Editor: Michele Iafisco

Copyright © 2016 Y. Y. Wang et al. This is an open access article distributed under the Creative Commons Attribution License, which permits unrestricted use, distribution, and reproduction in any medium, provided the original work is properly cited.

In order to investigate the relationship between induction heating ability of Fe_2O_3 -CaO-SiO₂ glass ceramics and chemical composition, a series of glass ceramic samples with different chemical compositions were prepared by the sol-gel method. The structural, textural, and magnetic properties of the samples were analyzed and correlated with the Fe_2O_3 content. This is the first time work of its kind that evaluates the relationships between induction heating ability and chemical composition of Fe_2O_3 -CaO-SiO₂ glass ceramics. The results showed that induction heating ability of Fe_2O_3 -CaO-SiO₂ glass ceramics increased gradually with increasing magnetite content. Also, the induction heating ability became considerably better when a small amount of phosphorus was introduced. This study thus reveals a methodology to control the induction heating ability of Fe_2O_3 -CaO-SiO₂ glass ceramics through modifying the chemical composition.

1. Introduction

Magnetic induction hyperthermia has been found to be a useful modality for cancer therapy recently and the thermoseed materials used in hyperthermia therapy have become a topic of increasing research focus [1–3]. The thermoseed material must be biocompatible and contain a magnetic phase to generate and dissipate the proper amount of heat under alternating magnetic fields. Ferromagnetic and bioactive glass ceramics are considered to be effective thermoseed materials for cancer therapy. In particular, Fe_2O_3 -CaO-SiO₂ glass ceramics are of great interest to researchers, due to their excellent magnetic properties and good biological activity. Several Fe_2O_3 -CaO-SiO₂ glass ceramics having a considerable amount of magnetic phases have been developed for this application [4–7]. In fact, hyperthermic cancer therapy using Fe_2O_3 -CaO-SiO₂ ferromagnetic glass ceramics has already been reported to show excellent results in animal experiment [8–10].

Fe_2O_3 -CaO-SiO₂ glass ceramics absorb magnetic energy and generate heat under the alternating magnetic field, as a result of eddy currents, Néel losses, and hysteresis losses [11–13]. There are several factors that influence the heat production rate [14], including the internal factors such as

permeability, magnetic energy product, material size, and microstructure, as well as external factors such as magnetic field frequency and amplitude. The magnetic property was found to be one of the most significant factors affecting the induction heating ability of glass ceramics. Lee et al. explored the effect of the iron state on crystallization in Fe_2O_3 -CaO-SiO₂ glasses [15], while Bretcanu et al. investigated the influence of crystallized Fe_3O_4 on magnetic properties of ferromagnetic glass ceramics [16]. Magnetic properties of CaO-P₂O₅-Na₂O- Fe_2O_3 -SiO₂ glass upon heat treatment were also analyzed by Shankhwar et al. [17]. However, to date, the effects of chemical compositions on the induction heating ability of Fe_2O_3 -CaO-SiO₂ glass ceramics have not been reported.

The Fe_2O_3 -CaO-SiO₂ glass ceramics with different compositions were prepared by the sol-gel method in this work. A small amount of phosphorus was introduced to increase the biological activity at the same time. Magnetic properties of the glass ceramic samples were evaluated and correlated mainly with the iron oxide content. The effect of Fe_2O_3 content on the induction heating ability of Fe_2O_3 -CaO-SiO₂ glass ceramics has been investigated by analyzing the crystal phase and magnetic properties of the samples. This study also reveals a methodology to control the magnetic properties

TABLE 1: Chemical compositions of different glass ceramic samples (wt%).

Sample	Fe ₂ O ₃	CaO	SiO ₂	P ₂ O ₅
A1S1	15	42	43	0
A1S3	20	39	41	0
A1S5	25	36	39	0
A1S7	30	34	36	0
A1S9	35	32	33	0
A2P1	30	39	30	1
A2P7	28	37	28	7

of Fe₂O₃-CaO-SiO₂ glass ceramics through the chemical composition and its potential application in hyperthermia treatment of cancer.

2. Materials and Methods

2.1. Preparation of Fe₂O₃-CaO-SiO₂ Glass Ceramics. Several different Fe₂O₃-CaO-SiO₂ glass ceramics samples were prepared by the sol-gel method and classified as groups A1 and A2 (without phosphorous and with phosphorous, resp.).

The chemical compositions of the samples are shown in Table 1. The dosages of reagents calculated on the base of the chemical compositions were listed in Table 2. Briefly, the procedure involved preparing a solution of tetraethyl orthosilicate (TEOS) in ethanol. Distilled water was added to the solution such that the molar ratio of TEOS and water was 1:15. Then hydrochloric acid was added to the solution and stirred with a magnetic stirrer for 10 min, and then calcium nitrate and iron nitrate were added to the solution. Triethyl phosphate was also added to the solution in group A2 at this time. The resulting solution was placed in a water bath at 45°C for 150 min. Then the temperature was raised up to 65°C until the solution became semisolid. The samples were aged for 7 days at room temperature, and the gels obtained were baked in the drying oven at 120°C for 12 h. Finally, the dried samples were heated to 650°C for an hour, followed by further heating at 950°C for 1 hour in a heat treatment furnace in a reducing atmosphere. The glass ceramic samples thus obtained were cooled to room temperature and characterized as described in the following sections.

2.2. Characterization. X-ray diffraction (XRD) analysis was performed with a XD-6 X-ray diffractometer at room temperature, with CuK α radiation, 36 kV voltage, and 20 mA current. X-ray data were collected in the $5 < 2\theta < 80$ range. Prior to the XRD test, the samples were ground into powder and sieved through a 300-mesh gauze.

Microarea elemental compositions of the samples were determined using a scanning electron microscopy (SEM) system (S-3400N) equipped with energy dispersive spectrometer (EDS). The samples were coated with a layer of gold approximately 10 nm thick, and the samples were analyzed for a live time of 30 s. The total amounts of oxide in the samples were normalized to 100%, and the Fe²⁺ and Fe³⁺ contents were converted to the equivalent Fe₂O₃ content.

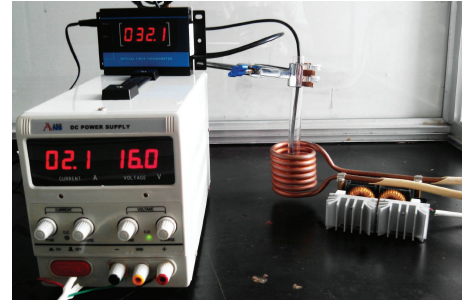


FIGURE 1: Homemade device for measuring induction heating ability.

Magnetization measurements were performed using a vibrating sample magnetometer (VSM, Lakeshore model 7407) at room temperature.

A homemade device was built for measuring the induction heating ability (Figure 1). The glass ceramics samples were introduced into a copper coil, which was part of a resonant RLC circuit producing an AC magnetic field in the frequency range 80 kHz–100 kHz and with amplitudes up to 0.15 kA/m. The copper coil was cooled by circulating water, and the temperature was monitored using a fiber thermometer placed in the center of the sample. The induction heating ability was determined by plotting the initial linear rise in temperature versus time, normalized to the mass of the sample.

3. Results and Discussion

3.1. Crystal Phase Analysis. XRD patterns of the glass ceramic samples of group A1 are shown in Figure 2(a), demonstrating the presence of a mixture of crystalline phases for all the materials. Three major crystalline phases, wollastonite (JCPDS No. 84-0654), magnetite (JCPDS No. 85-1436), and hematite (JCPDS No. 85-0599) were observed in group A1 samples. The hematite level of sample A1S9 was much higher than those of other samples. XRD patterns of the glass ceramic samples of group A2 with phosphorous were characterized by the major hydroxyapatite phase (JCPDS No. 09-0432) in addition to the above three major crystalline phases (Figure 2(b)). Hydroxyapatite is the main constituent of bones, and the presence of this bone mineral phase along with the magnetic phase suggests both the biocompatible nature and the induction heating ability of the samples.

The relative mass of each phase, which was also calculated according to the XRD patterns, was listed in Table 3. The amounts of both magnetite and hematite phase of group A2 were more than that of group A1, and the increase of magnetite content indicates that the induction heating ability would get stronger.

3.2. Chemical Composition Analysis. The SEM-EDS spectra for the samples are shown in Figure 3. The results confirmed the presence of silicon, calcium, and iron in samples A1S5 and A1S7 while silicon, phosphorus, calcium, and iron were present in all the samples of group A2. Samples A1S5 and A1S7

TABLE 2: The amount of the reagent.

Sample	Iron nitrate (g)	Calcium nitrate (g)	TEOS (mL)	Triethyl phosphate (mL)	Ethanol (mL)
A1S1	3.62	8.43	7.60	0	22.80
A1S3	4.82	7.83	7.25	0	21.74
A1S5	6.03	7.22	6.89	0	20.68
A1S7	7.23	6.82	6.36	0	19.09
A1S9	8.44	6.42	5.83	0	17.50
A2P1	7.23	8.03	5.30	0.12	15.91
A2P7	6.75	7.59	4.82	0.76	14.46

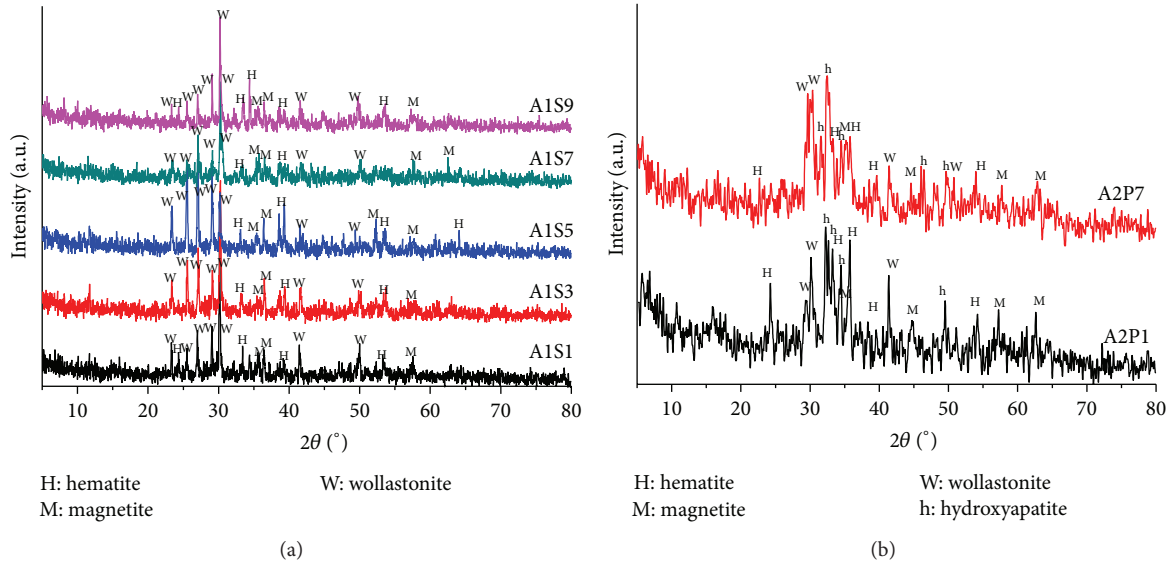


FIGURE 2: Room temperature XRD patterns of glass ceramic samples.

TABLE 3: The relative mass of the phases of the samples (wt%).

Sample	Hematite	Magnetite	Wollastonite	Hydroxyapatite
A1S1	4.7	2.8	92.5	0
A1S3	2.5	2.6	94.8	0
A1S5	2.4	1.6	96.1	0
A1S7	3.8	4.8	91.4	0
A1S9	5.9	4.2	89.9	0
A2P1	15	6	45.1	33.9
A2P7	7.5	4.5	50	38

showed the presence of lathlike particles while the mineral particles in group A2 were granular. Moreover, the particle sizes of A2P1 were about $3 \mu\text{m}$, which was much smaller than that of A1S7 which was about $16 \mu\text{m}$. The chemical compositions of the samples calculated from EDS are given in Table 4. No other elements were identified, which ruled out the influence of impurities on the induction heating ability of the samples.

3.3. Magnetic Properties. Figure 4 shows the magnetization (M - H) curves obtained for the samples as a function of applied magnetic field. The samples exhibit hysteresis with

TABLE 4: Chemical composition of the samples determined by SEM-EDS (wt%).

	Fe_2O_3	CaO	SiO_2	P_2O_5
A1S5	28.71	37.75	33.54	0
A1S7	22.73	32.79	45.01	0
A2P1	32.57	34.26	30.40	2.76
A2P7	32.05	30.95	25.31	11.70

narrow hysteresis loop and low coercivity, suggesting the soft ferromagnetic nature of the samples. This is due to the formation of the magnetic phase upon heat treatment, as already confirmed by the XRD results.

The different magnetic parameters of the samples are listed in Table 5. Sample A1S7 shows higher saturation magnetization M_s (19 emu/g) and remanent magnetization M_r (2.3 emu/g) than the other samples of group A1. This may be due to the enhancement in the magnetic phase in A1S7. However, M_s and M_r values began to decrease when the Fe_2O_3 content was over 30% (Figure 5), which can be attributed to the higher hematite content and the lower magnetite content. A2P1 has a lower saturation magnetization value but a larger coercive force compared to A1S7. The lower saturation magnetization may be attributed to some possible reactions

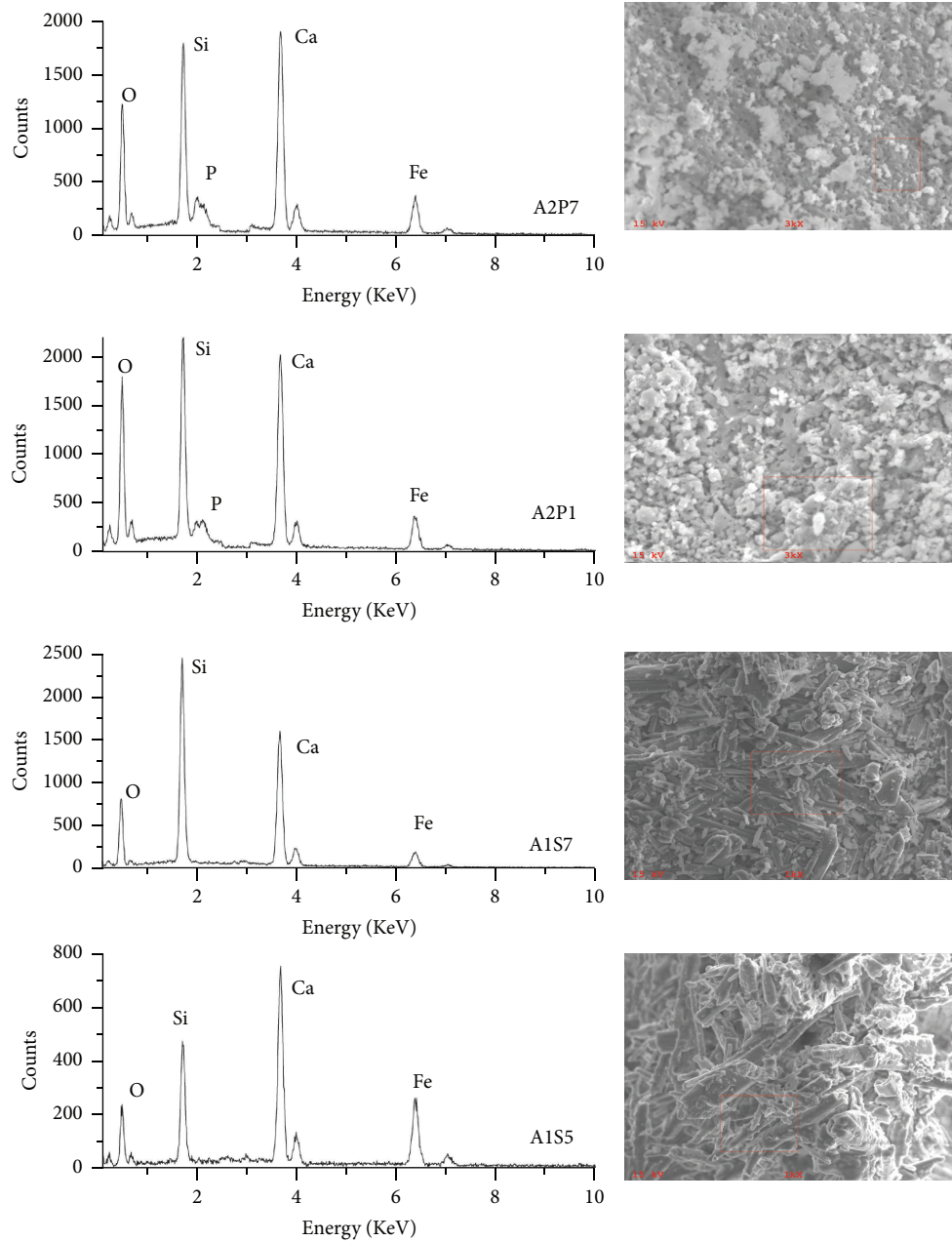


FIGURE 3: SEM-EDS spectra and images of the samples.

TABLE 5: Magnetic parameters of the samples.

	A1S1	A1S3	A1S5	A1S7	A1S9	A2P1	A2P7
H_c (G)	147.76	124.82	206.83	106.24	82.45	113.85	87.87
M_s (emu/g)	1.99	2.06	3.32	19	17.09	10.99	10.65
M_s^* (emu/g)	13.27	10.30	13.28	63.33	48.83	36.63	38.04
M_r (emu/g)	0.33	0.41	0.60	2.30	0.78	2.25	3.04
Interpolated hysteresis area	65649	176034	287151	1683193	525486	923229	980057

Note: M_s values were normalized to the total weight of the sample; M_s^* values were normalized to the weight of Fe_2O_3 component alone.

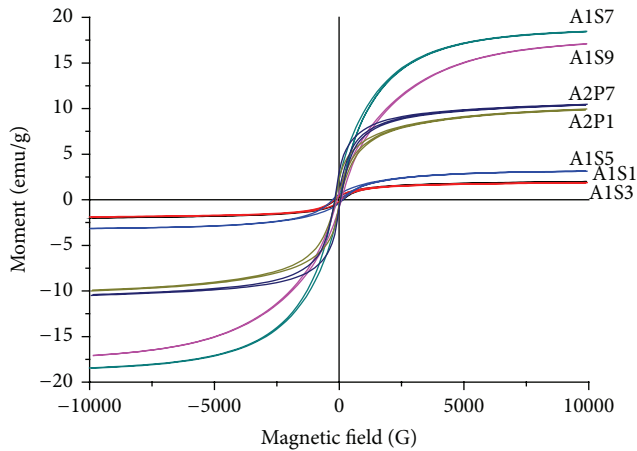


FIGURE 4: M - H curves of the glass ceramic samples with different chemical composition.

during the heating process. It is a known fact that P_2O_5 and SiO_2 can easily react with Fe_2O_3 forming nonmagnetic phases at high temperature [18]. Also, Fe could enter into the crystalline structure forming a solid solution [19]. The coercive field was also influenced in a significant way by the crystal dimensions [20]. The SEM results showed that the average crystallite size of A2P1 was smaller than that of A1S7. The smaller crystallite size of the magnetic phase results in a larger coercive force. These observed phenomena were similar to previous reports [21].

Figure 5 shows the relationship between the different magnetic parameters and Fe_2O_3 content of the samples. The integrated hysteresis loop area was calculated for a maximum applied field of 10000 G. The relationship between integrated loop area and the Fe_2O_3 content was similar to that observed in the case of saturation magnetization. It can be seen from Figure 5 that the hysteresis loop area of A1S7 with 30% Fe_2O_3 content is much larger than that of the other samples in group A1, which may be attributed to the higher remanence of A1S7. Theoretically, the energy generated by the glass ceramic samples under low magnetic field can be estimated from the hysteresis loop area [6]. Thus, the above results indicate that A1S7 should be capable of generating a larger amount of heat than the other samples, under a proper alternating magnetic field.

3.4. Induction Heating Ability. To test the heating ability of the samples, the induction heating experiments were performed with the different samples. Hyperthermia heating curves, measured at a fixed current of 2 A for 11 min with 1 g concentrations of the samples, are shown in Figure 6. The heating rates of the samples were basically the same, and the temperature increased rapidly until 10 min. The temperature variation amplitudes of the samples were found to increase gradually with the increase of Fe_2O_3 content of the samples. However, the induction heating ability began to fall when the Fe_2O_3 content was over 30%, which may be caused by the lower magnetite content. Sample A1S7 showed the largest temperature variation amplitudes of $2.7^\circ C$ in group A1, which is consistent with the results in previous sections. More interestingly, the temperature variation amplitudes of all the

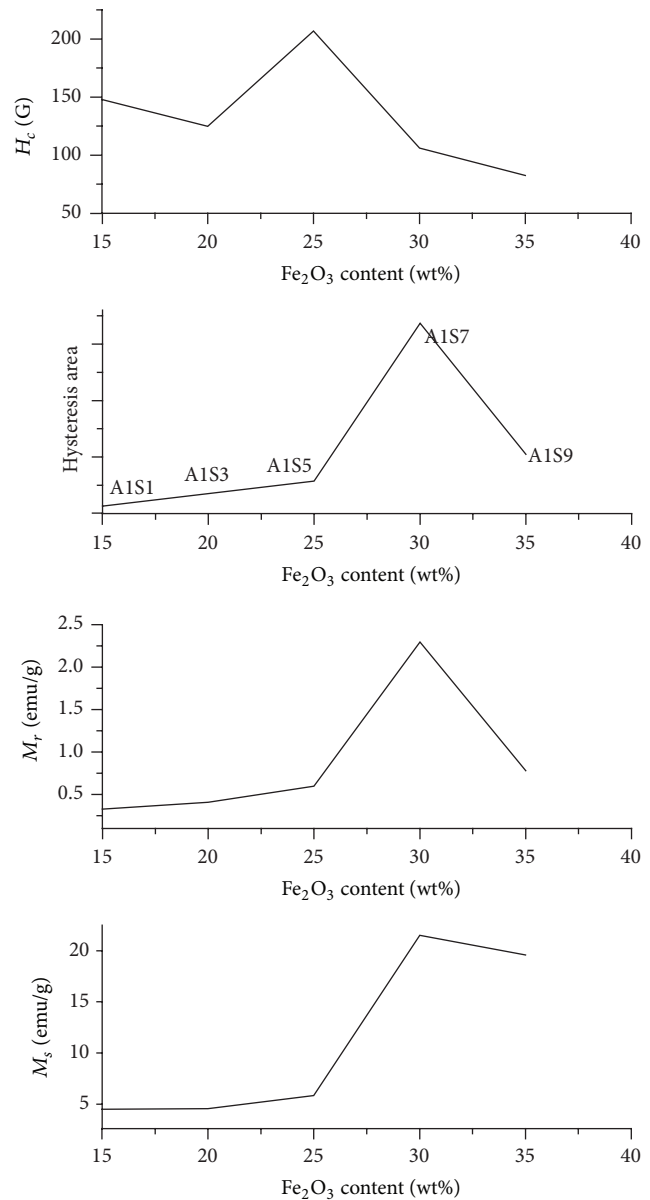


FIGURE 5: Relationship between magnetic properties and the Fe_2O_3 content.

samples in group A1 were about $2^\circ C$, while the temperature variation amplitudes of the samples in group A2 with phosphorus were as high as $15^\circ C$. The addition of phosphorus not only changed the crystalline phase of the samples but also significantly increased their induction heating ability. These results indicate that P_2O_5 - Fe_2O_3 - CaO - SiO_2 glass ceramics are more suitable for hyperthermia treatment than Fe_2O_3 - CaO - SiO_2 glass ceramics.

In ferromagnetic materials, heat generation is mainly due to hysteresis loss. In addition, other physical parameters such as particle size and distribution of the components, as well as magnetic field intensity, also considerably influence the heating properties under AC magnetic field. The effect of these factors may be the reason for the ability of group A2 samples to generate more heat than group A1 samples.

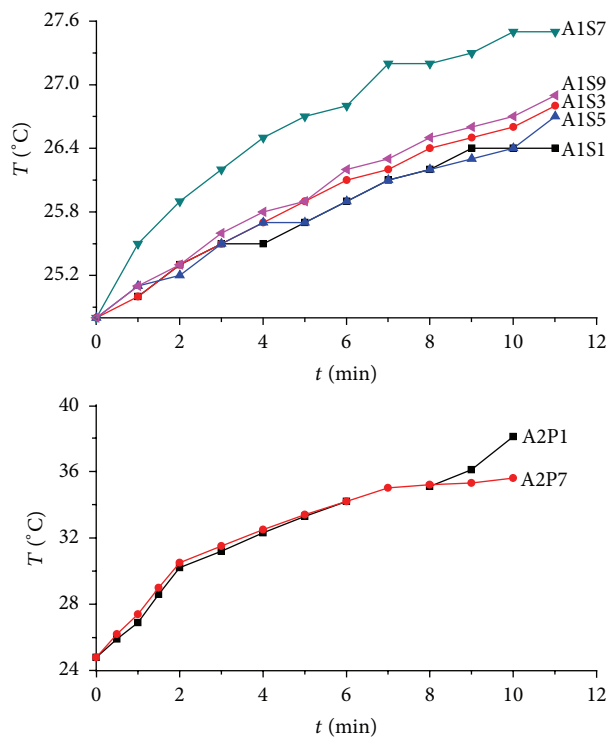


FIGURE 6: Temperature evolution as a function of time in the hyperthermia tests.

Further work is in progress in our laboratory to understand the heating properties of this class of glass ceramics and to optimize the composition for therapeutic application.

4. Conclusions

$\text{Fe}_2\text{O}_3\text{-CaO-SiO}_2$ glass ceramics of different compositions were prepared by the sol-gel method and tested for their induction heating ability. Magnetic properties of the glass ceramic samples were found to correlate with the Fe_2O_3 content. The saturation magnetization and the integrated loop area increased with the magnetite content in A1 group. Thus, the induction heating ability of A1S7 sample was the strongest among all the prepared $\text{Fe}_2\text{O}_3\text{-CaO-SiO}_2$ glass ceramics. Moreover, the induction heating ability was significantly improved when a small amount of phosphorus was introduced into the $\text{Fe}_2\text{O}_3\text{-CaO-SiO}_2$ glass ceramics. This reveals a promising methodology to control the magnetic properties of $\text{Fe}_2\text{O}_3\text{-CaO-SiO}_2$ glass ceramics through the chemical composition and its potential applications in hyperthermia treatment of cancer.

Competing Interests

The authors declare that they have no competing interests.

Acknowledgments

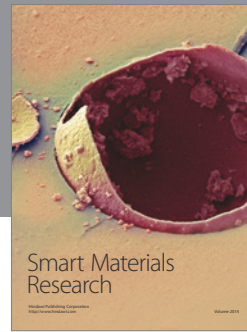
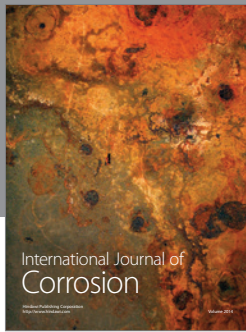
This research was financially supported by Natural Science Foundation for Youths of Zhejiang Province (LQ16E020001),

National Natural Science Foundation of China (no. 51372081), and Natural Science Foundation of Zhejiang Province (LY13E020006).

References

- [1] P. Moroz, S. K. Jones, and B. N. Gray, "Magnetically mediated hyperthermia: current status and future directions," *International Journal of Hyperthermia*, vol. 18, no. 4, pp. 267–284, 2002.
- [2] P. Wust, B. Hildebrandt, G. Sreenivasa et al., "Hyperthermia in combined treatment of cancer," *The Lancet Oncology*, vol. 3, no. 8, pp. 487–497, 2002.
- [3] L. Treccani, T. Yvonne Klein, F. Meder, K. Pardun, and K. Rezwan, "Functionalized ceramics for biomedical, biotechnological and environmental applications," *Acta Biomaterialia*, vol. 9, no. 7, pp. 7115–7150, 2013.
- [4] Y. Ebisawa, F. Miyaji, T. Kokubo, K. Ohura, and T. Nakamura, "Bioactivity of ferrimagnetic glass-ceramics in the system $\text{FeO-Fe}_2\text{O}_3\text{-CaO-SiO}_2$," *Biomaterials*, vol. 18, no. 19, pp. 1277–1284, 1997.
- [5] E. Ruiz-Hernández, M. C. Serrano, D. Arcos, and M. Vallet-Regí, "Glass-glass ceramic thermoseeds for hyperthermic treatment of bone tumors," *Journal of Biomedical Materials Research A*, vol. 79, no. 3, pp. 533–543, 2006.
- [6] R. K. Singh, A. Srinivasan, and G. P. Kothiyal, "Evaluation of $\text{CaO-SiO}_2\text{-P}_2\text{O}_5\text{-Na}_2\text{O-Fe}_2\text{O}_3$ bioglass-ceramics for hyperthermia application," *Journal of Materials Science: Materials in Medicine*, vol. 20, no. 1, pp. S147–S151, 2009.
- [7] Y. Y. Wang, B. Li, and Y. Y. Wang, "Characterization of $\text{Fe}_2\text{O}_3\text{-CaO-SiO}_2$ glass ceramics prepared by sol-gel," *Applied Mechanics and Materials*, vol. 624, pp. 114–118, 2014.
- [8] Y.-K. Lee, S.-B. Lee, Y.-U. Kim et al., "Effect of ferrite thermoseeds on destruction of carcinoma cells under alternating magnetic field," *Journal of Materials Science*, vol. 38, no. 20, pp. 4221–4233, 2003.
- [9] M. Matsumoto, N. Yoshimura, Y. Honda, M. Hiraoka, and K. Ohura, "Ferromagnetic hyperthermia in rabbit eyes using a new glass-ceramic thermoseed," *Graefes Archive for Clinical and Experimental Ophthalmology*, vol. 232, no. 3, pp. 176–181, 1994.
- [10] A. Matsumine, K. Kusuzaki, T. Matsubara et al., "Novel hyperthermia for metastatic bone tumors with magnetic materials by generating an alternating electromagnetic field," *Clinical and Experimental Metastasis*, vol. 24, no. 3, pp. 191–200, 2007.
- [11] P. R. Stauffer, T. C. Cetas, A. M. Fletcher et al., "Observations on the use of ferromagnetic implants for inducing hyperthermia," *IEEE Transactions on Biomedical Engineering*, vol. 31, pp. 76–90, 1984.
- [12] S. Mornet, S. Vasseur, F. Grasset, and E. Duguet, "Magnetic nanoparticle design for medical diagnosis and therapy," *Journal of Materials Chemistry*, vol. 14, no. 14, pp. 2161–2175, 2004.
- [13] Y. Ebisawa, F. Mijaji, T. Kokubo et al., "Bioactivity of ferromagnetic glass-ceramics in the system $\text{FeO-Fe}_2\text{O}_3\text{-CaO-SiO}_2$," *Biomaterials*, vol. 18, no. 19, pp. 1277–1284, 1997.
- [14] O. Bretcanu, E. Verné, M. Coisson, P. Tiberto, and P. Allia, "Magnetic properties of the ferrimagnetic glass-ceramics for hyperthermia," *Journal of Magnetism and Magnetic Materials*, vol. 305, no. 2, pp. 529–533, 2006.
- [15] Y.-K. Lee, K.-N. Kim, S.-Y. Choi, and C.-S. Kim, "Effect of iron state on crystallization and dissolution in $\text{Fe}_2\text{O}_3\text{-CaO-SiO}_2$ glasses," *Journal of Materials Science: Materials in Medicine*, vol. 11, no. 8, pp. 511–515, 2000.

- [16] O. Bretcanu, S. Spriano, E. Verné, M. Cöisson, P. Tiberto, and P. Allia, "The influence of crystallised Fe_3O_4 on the magnetic properties of coprecipitation-derived ferrimagnetic glass-ceramics," *Acta Biomaterialia*, vol. 1, no. 4, pp. 421–429, 2005.
- [17] N. Shankhwar, G. P. Kothiyal, and A. Srinivasan, "Understanding the magnetic behavior of heat treated $\text{CaO-P}_2\text{O}_5\text{-Na}_2\text{O-Fe}_2\text{O}_3\text{-SiO}_2$ bioactive glass using electron paramagnetic resonance studies," *Physica B*, vol. 448, pp. 132–135, 2014.
- [18] Z. Zhigang, *Ferrite Magnetic Material*, Science Press, Beijing, China, 1981.
- [19] Y. Ohashi and L. W. Finger, "The role of octahedral cations in pyroxenoid crystal chemistry. I. Bustamite, wollastonite, and the pectolite-schizolite-serandite series," *American Mineralogist*, vol. 63, pp. 274–288, 1978.
- [20] S. Chikazumi, S. Taketomi, M. Ukita et al., "Physics of magnetic fluids," *Journal of Magnetism and Magnetic Materials*, vol. 65, no. 2-3, pp. 245–251, 1987.
- [21] R. K. Singh and A. Srinivasan, "Bioactivity of ferrimagnetic $\text{MgO-CaO-SiO}_2\text{-P}_2\text{O}_5\text{-Fe}_2\text{O}_3$ glass-ceramics," *Ceramics International*, vol. 36, no. 1, pp. 283–290, 2010.



Hindawi

Submit your manuscripts at
<http://www.hindawi.com>

